

Modeling of Interstitial Microwave Hyperthermia for Hepatic Tumors Using Floating Sleeve Antenna

Faihaa Eltigani

University of Gezira

Sulafa Ahmed (✉ sulafa174@gmail.com)

University of Gezira <https://orcid.org/0000-0003-2237-8891>

Maged Yahya

University of Gezira

Mawahib Ahmed

University of Gezira

Research Article

Keywords: Liver tumor, microwave hyperthermia, sleeve antenna, Pennes' equation, metabolic rate, SAR

Posted Date: January 13th, 2022

DOI: <https://doi.org/10.21203/rs.3.rs-900511/v2>

License: © ⓘ This work is licensed under a Creative Commons Attribution 4.0 International License.

[Read Full License](#)

Version of Record: A version of this preprint was published at Physical and Engineering Sciences in Medicine on April 15th, 2022. See the published version at <https://doi.org/10.1007/s13246-022-01124-4>.

Modeling of Interstitial Microwave Hyperthermia for Hepatic Tumors Using Floating Sleeve Antenna

Faihaa Eltigani^{1†}, Sulafa Ahmed^{1†*}, Maged Yahya¹ and Mawahib Ahmed¹

*Correspondence:
Sulafa174@gmail.com
1Department of
Electronic Engineering
University of Gezira,
Sudan
†Equal contributors

Abstract

Purpose: Microwave hyperthermia is a treatment modality that uses microwaves to destroy cancer cells by increasing their temperature to 41-45°C. This study aims to design, modeling, and simulation of a microwave sleeve antenna for hepatic (liver) hyperthermia.

Method: The designed antenna resonated at 2.45 GHz. The antenna was tested in six different 3D liver models: Model A: without a tumor and blood vessels; Model B: with a realistic tumor (2×3 cm) and without blood vessels; Model C: created by adding blood vessels to model B; Model D: created by adding a small tumor (1.5×1.5 cm) to model C and changed its location; Model E: same as model C with a different tumor size; Model F: model with a simple spherical tumor (1.5×1.5 cm).

Results: The return loss of the antenna varied from -45 dB to -25 dB for the 6 models. The Specific Absorption Rate (SAR) was between 29 W/kg to 30W/kg in the tumors and below 24 W/Kg in the surrounding tissues. The tumors' temperature elevated to 43- 45°C, while the temperature of the surrounding tissues was below 41°C.

Conclusions: The results showed the capability of the designed antenna to raise the temperature of hepatic tumors to the therapeutic ranges of hyperthermia.

Keywords: Liver tumor, microwave hyperthermia, sleeve antenna, Pennes' equation, metabolic rate, SAR.

Introduction

According to the American Cancer Society, liver (Hepatic) cancer has an estimated 42,230 new cases in 2021 and about 30,230 cases are expected to die of this cancer. Approximately 80% of these cases occur in developing countries [1]. Currently, surgical resection is a standard treatment for liver cancer since it provides survival benefits. Patients did not well accept chemotherapy and radiotherapy because of their side effects [2]. Only 5–15% of hepatic tumors could undergo such curative surgery [2], because of: multifocal disease, tumor size, and location in relation to key blood vessels. For these reasons, there is an emergent need for interstitial techniques for the treatment of hepatic tumors, such as microwave hyperthermia (MWH). In a microwave hyperthermia, an applicator is inserted into the tumor to raise its temperature to 41-45°C without damaging the surrounding normal tissues [3, 4].

Microwave hyperthermia uses microwave-generated heat to shrink or destroy tumors [2]. The simple devices to perform an interstitial microwave hyperthermia comprised of a microwave generator, a microwave applicator/antenna, and a flexible coaxial cable to connect the antenna to the microwave generator [4]. Using these thin microwave hyperthermia devices has many advantages: avoiding the possible damage of surrounding tissues and reducing the procedural risks [5].

Many studies designed microwave sleeve antennas for hepatic microwave hyperthermia using simple models of both tumors and livers-which did not reflect the actual effect of the anatomical structures and blood circulation on the temperature distribution [5-10]. This work aims to design a microwave sleeve antenna capable of heating hepatic tumors using realistic 3D liver and tumor models.

Method

Antenna design

We designed an antenna of 3.4 mm in diameter from a 50Ω coaxial cable with inner and outer conductors made of copper. We used Teflon as a dielectric material

between the conductors. In addition, we used it as a catheter for easy insertion and removal of the antenna. We chose the antenna geometry parameters, slot spacing, and floating sleeve length based on the effective wavelength in human liver tissue at 2.45 GHz. We used Equation 1 for calculation [7]:

$$\lambda_{\text{eff}} = \frac{c}{f\sqrt{\epsilon_r}} \quad (1)$$

Where c is the speed of light in free space, f is the operating frequency of the microwave generator (2.45 GHz), and $\epsilon_r = 43.03$ is the relative permittivity of human liver tissue at 2.45 GHz; this yielded the effective wavelength of approximately 18.667 mm.

Slot spacing, floating sleeve length corresponds to $0.25 \lambda_{\text{eff}}$, and λ_{eff} respectively, which are chosen and then optimized to achieve localized power deposition near the distal tip of the antenna. **Figure 1** shows the schematic diagram of the designed floating sleeve antenna (dimensions in mm), and **Table 1** shows the layers' dimensions.

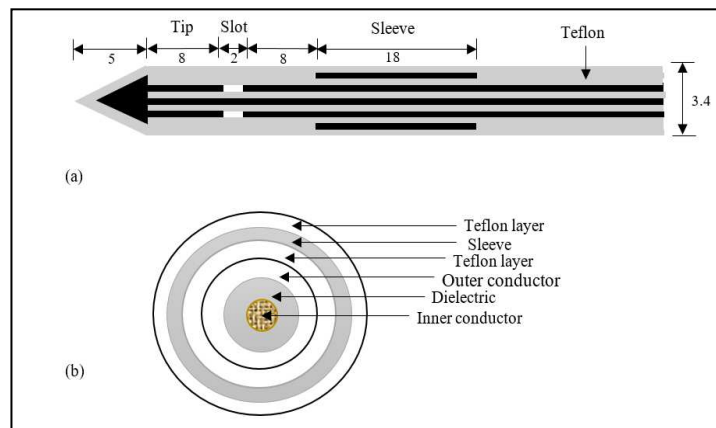


Figure1. Geometry of the floating sleeve antenna; (a) Schematic diagram of the antenna; (b) Antenna cross-section at the sleeve

Table 1. Dimensions of the sleeve antenna

Dimension	Value (mm)
Diameter of the inner conductor	0.5
Diameter of the Teflon	1.63
Diameter of outer conductor	1.79
Inner diameter of the sleeve	2.5
Outer diameter of the sleeve	3.2
Diameter of the inner tip	2.6
Diameter of the outer tip	3.4

In the antenna design, the pattern of a linear dipole with an overall length less than the half-wavelength ($L < \lambda/2$) is insensitive to the frequency [11]. Thus, we chose the dipole length to be greater than the half-wavelength according to Equation 2.

$$\lambda = \frac{c}{f} \quad (2)$$

Where c is the speed of light in free space and f is the operating frequency of the microwave generator (2.45 GHz), this resulted in a half-wavelength of 61.18mm.

We used The Computer Simulation Technology (CST) software[12] to simulate antenna design and its interactions with the liver tissues

The Original Liver Model

The original model is a realistic 3D model (from the 3D-IRCADb-01 database) of a man's liver with blood vessels and a tumor (2×3 cm) [13]. This model was used to generate six models.

Assigning material properties

We assigned the electrical and thermal properties for liver tissues according to the literature and the CST material library [7, 8, 14-23]. Assigning the metabolic properties was one of the major challenges because of lacking of reported values for the basal metabolic rate (BMR) of hepatic tumors. The literature cites the changing of

tumors' metabolic activities compared to the normal cells. These changes support the acquisition and maintenance of malignant properties [24]. Gorbach *et al.* reported that brain tumors have 0.5 to 2 °C higher temperatures than surrounding tissues [25]. In addition, Mital *et al.* measured the elevation of skin temperature over breast tumors to 2-3°C above the normal skin temperatures [16]. The liver has a higher metabolic rate than the breast and brain [26]; based on this, we chose the BMR of the tumor to be 10 times the surrounding tissues (120000 W/m³), with 3400 W/m³/K as a perfusion rate. Table 2 presents assigned material properties.

Table 2: Material properties for liver and tumor at 2.45 GHz

Property	Liver	Blood	Tumor
Relative permittivity (ϵ_r)	43.03	58.30	48.16
Electrical conductivity (σ)	1.69	2.54	2.09
Density (ρ)	1060	1000	1045
Specific heat capacity (c^b)	3600	4180	4200
Thermal conductivity (k)	0.512	0.49	0.60
Blood flow coefficient	68000	1e+006	3400
BMR	12000	-	120000

The temperature elevation in this study was based on Pennes' suggestion (Equation3)

$$\rho c \frac{\partial T}{\partial t} = k \frac{\partial^2 T}{\partial x^2} + k \frac{\partial^2 T}{\partial y^2} + k \frac{\partial^2 T}{\partial z^2} + w_b c_b (T_a - T) + Q_m + Q_r(x, y, z, t) \quad (3)$$

Where $T = T(x, y, z, t)$ is the temperature elevation (°C), ρ the physical density of the tissue (kg/m³), c the specific heat of the tissue (J/kg/°C), k the tissue thermal conductivity (W/m°C), w_b the blood volumetric perfusion rate (kg/m³/s), c_b the specific heat of blood (J/kg/°C), and $T_a = T_a(x, y, z, t)$ the average temperature elevation of the arteries (°C). Q_m is the mechanism for modeling physiological heat generation (W/m³) and Q_r the regional heat delivered by the source (W/m³). The term $w_b c_b (T_a - T)$, which is the perfusion heat loss (W/m³), is always considered in with tissues which have high degree of perfusion, such as a liver. In general, w_b is

assumed to be uniform throughout the tissue. However, its value may increase with heating time because of vasodilation and capillary recruitment [2].

The complete system (antenna and liver) simulation

The antenna was designed in CST MICROWAVE STUDIO, then the liver model was imported and the materials' properties were assigned. The transient solver of CST MICROWAVE STUDIO was used to calculate the antenna parameters and the Specific Absorption Rate (SAR). Finally, the thermal solver in CST MPHYSICS STUDIO was used to solve the Pennes' bio-heat equation. The initial setting of the temperature was 25°C and 37°C for the surrounding ambient and tissues, respectively. We set open boundary conditions for both solvers. The simulation time was 10 minutes.

Figure 2 shows the complete system with different models. We tested the designed antenna first in a liver model without a tumor or blood vessels (Model A), then in a model with a tumor of about 2×3cm and with no blood vessels (Model B). After that, we tested the antenna in a complete model with the same tumor and blood vessels (Model C). To test the effect of both size and location of the tumor, we changed the location of the original tumor (Model D) and shrank it to (1.5×1.5cm) (Model E). Finally, we tested a model with a spherical tumor of 1.5 cm diameter (Model F). SAR and temperature were calculated for all models.

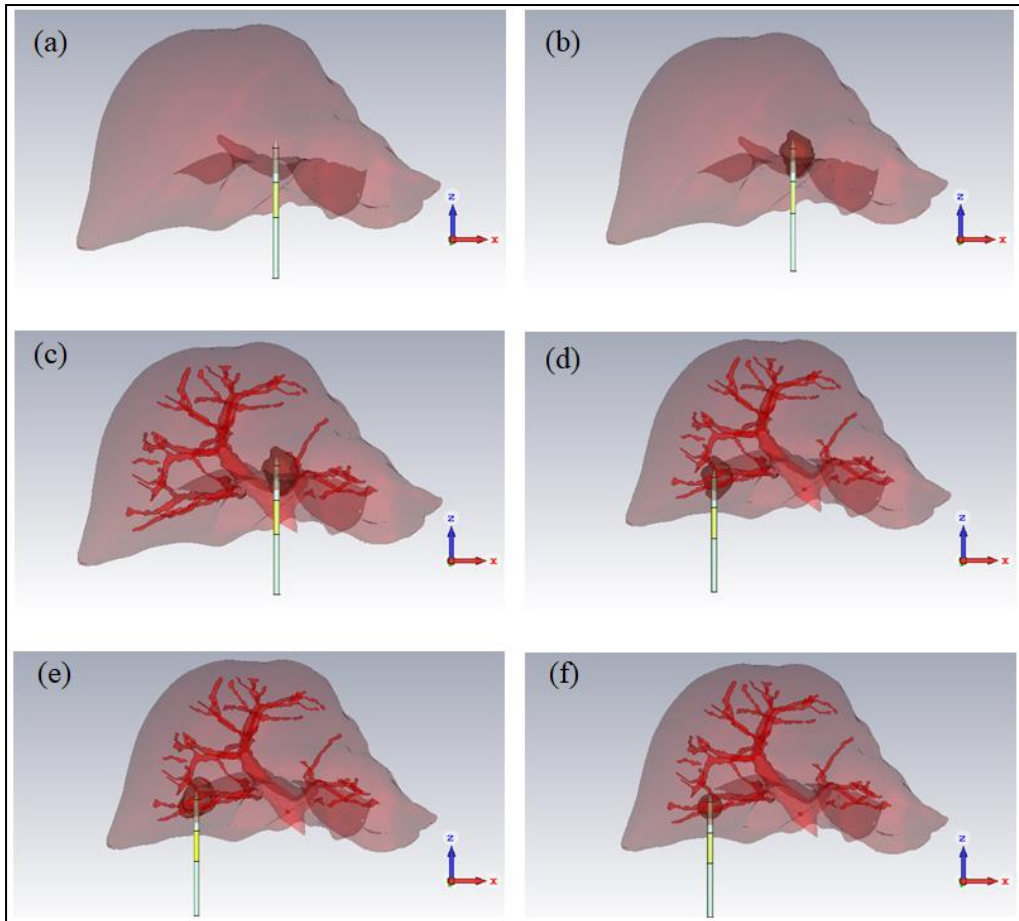


Figure 2. Liver models. (a) Model A (no tumor and blood vessels) (b) Model B (with tumor and without blood vessels). (c) Model C (Complete model with 2×3 cm tumor). (d) Model D (2×3 cm tumor at different locations). (e) Model E (smaller tumor about 1.5×1.5 cm). (f) Model F (1.5 X 1.5 cm spherical tumor).

Results

The antenna showed the capability of raising the temperature of hepatic tumors to above 41 °C, while the temperature of the surrounding tissues was below 41 °C. For each simulation model, the return loss, SAR and, temperature were calculated.

Return loss

Values of the return loss at 2.45 GHz varied from -45dB to -27 dB (**Figure 3**). It could be observed that the maximum value (-45dB) was obtained in model F (model with spherical tumor), and the minimum value (-27 dB) was obtained in model A (model without tumor and blood vessels).

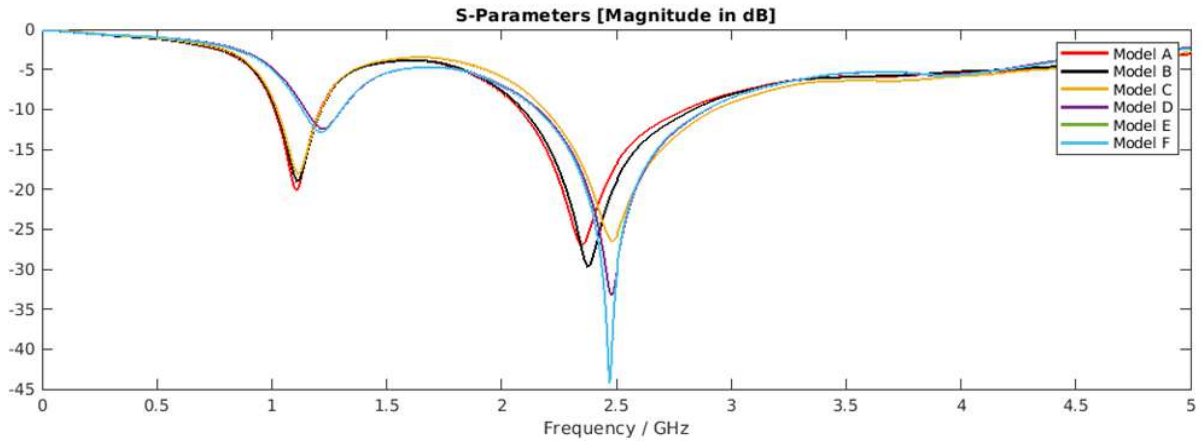


Figure 3. Return loss for antenna with different simulation models

Specific Absorption Rate (SAR)

The SAR value for the model with no tumor and blood vessels was 30.2 W/Kg (**Fig 4.a**), where the values varied from 31.4 W/Kg to 29.4 W/Kg for others models with tumors (**Figs 4.b-e**). In these models, we observed the high value in model B (without blood vessels) (**Fig 4.b**).

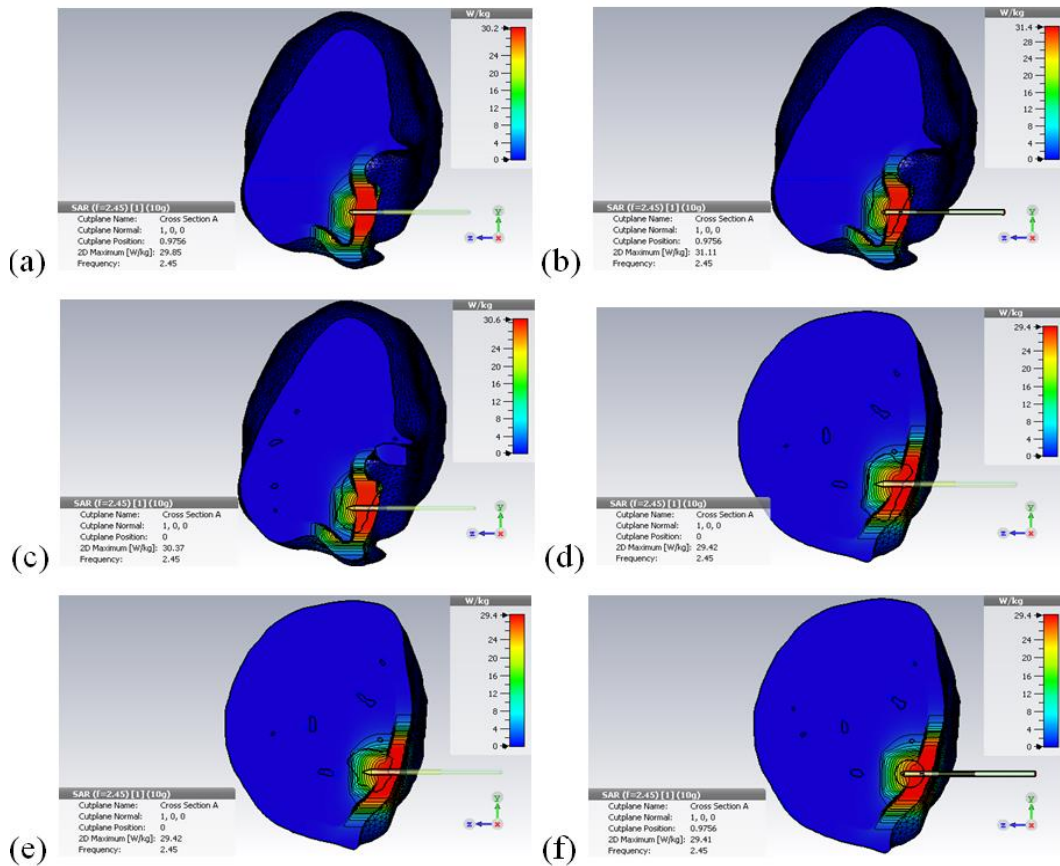


Figure 4. SAR distribution (a) SAR in model A, (b) SAR in model B, (c) SAR in model C, (d) SAR in model D, (e) SAR in model E, (f) SAR in model F

Temperature results

Considering that the SAR values alone are insufficient to access the hyperthermia effect, it is essential to calculate the temperature of the tumor and surrounding tissues.

Figure 6 shows the temperature pattern in all models. We observed that model A, where there is no tumor; the higher temperature was 39.7 °C which is below the hyperthermia range. For the other models, the temperature elevation in the tumors was within the therapeutic range (41- 45°C). Compared to other models with tumors (**Figures 5 b-e**), the temperature pattern in the model with the spherical tumor (**Fig 5.f**) showed a uniform distribution. Model C (**Fig 5. c**) showed the best results with the temperature reaching 45.6°C and uniform distribution within the tumor.

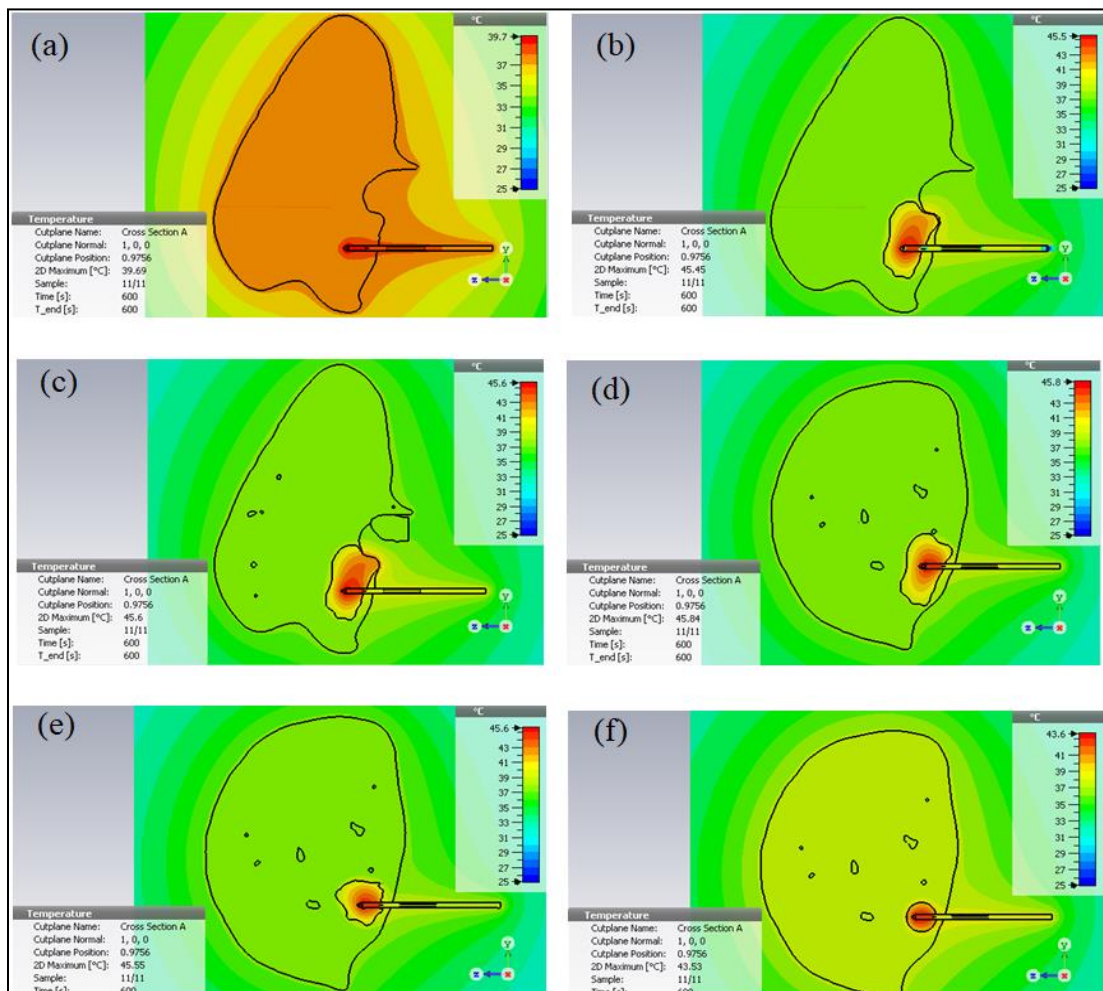


Figure 6. Temperature distribution (a) Model A. (b) Model B. (c) Model C. (d)

Model D. (e) Model E. (f) Model F

Discussion

This study introduced a design of a sleeve antenna for microwave hyperthermia. The antenna was tested in six liver models, and the return loss, SAR, and temperature were calculated. The results showed that the return loss values at 2.45 GHz (Figure 3) varied by changing tumor size and location. Compare the return loss values (-45dB to -27 dB) with other antennas designed for MWH; the current study has smaller values. Maini et al. got values of -24.8 dB at 2.45 GHz, while Chaichanyut *et al.* obtained -20 dB at 2.45GHz [5] and [23]. Since the efficiency of an antenna mainly depends on the antenna's return loss, small values show greater output power coupled to a tumor.

For the models with tumors, we observed high SAR values in the tumor placed at a model without blood vessels (**Fig 4. a**). This observation could be interpreted by the absence of the blood vessels (high conductivity tissues). In the other models, we recorded high SAR values in the tumor (**Figures 4. b-d**), which could be due to the proper localization of the designed antenna and the high conductivity of the tumor.

Considering that shape, volume, and surface area affect the amount of absorbed microwaves and subsequently energy focusing and overheating [27], it could observe that the SAR pattern in the model with the spherical tumor (**Fig 4.e**) showed uniform distribution and lower values compared to the realistic tumors. Many studies used simple models to test the performance of their applicators [5, 7-9], but the accuracy of their results was less than the accuracy obtained by using realistic models.

Based on the results of a model without a tumor (**Figure 5.a**), metabolic rate plays a fundamental role in raising the tumor temperature since the temperature was uniform in the complete model with a slight increase (1°C) around the tip of the antenna. Considering the assumptions of increasing tumor temperature from 0.5 to 3°C, the antenna elevates the tumor temperature to about 6°C. The presence of blood

vessels showed a direct effect on the temperature distribution (**Fig 5. a, b**), since the temperature decreased in the upper side of the tumor close to the lateral blood vessel. Many studies neglected the BMR effect and used SAR patterns to evaluate the efficiency of the designed applicator [10] [28].

Sajan Singh *et al.* [29] designed a coaxial antenna for MWH and tested its performance in a realistic liver model (without blood vessels). Compared to the proposed antenna, they obtained the required temperature for microwave hyperthermia after applying a power of up to 4W with a longer simulation time (up to 30 minutes), which reflected the potentiality of using a floating sleeve antenna for interstitial microwave hyperthermia applications. In future works, authors will enhance the antenna design to be smaller than the current one. In addition, test the antenna in a 3D model with more than one tumor in different locations.

Conclusion

In this study, an interstitial microwave hyperthermia antenna for hepatic tumors was designed. The antenna raised the tumors' temperature to the therapeutic values. The designed antenna worked properly with tumors with sizes of around 2×3 cm, while it can ablate tumors with larger size with over one hyperthermia session (with different insertion sites).

Declarations

Ethics approval and consent to participate

Not applicable.

Consent for publication

The participants acknowledged their consent to publish the acquired data.

Availability of data and materials

The used datasets are available from the corresponding author on reasonable request.

Competing interests

The authors declare that they have no competing interests.

Funding

This research did not receive any type of grants.

Authors' contributions

Faihaa Eltigani and Sulafa Ahmed carried out the concept, design of the study, interpreted the data and wrote the first manuscript. Mawahib Ahmed and Maged Yahya provided critical revision of the manuscript.

Acknowledgements

Not applicable.

Author's details

¹ Electronics Engineering Department, Faculty of Engineering and Technology, University of Gezira, Sudan.

References

1. American Cancer Society. *Key Statistics About Liver Cancer*. 2021 [08 September 2021]; Available from: <https://www.cancer.org/cancer/liver-cancer/about/what-is-key-statistics.html>.
2. Habash, R., *Bioeffects and therapeutic applications of electromagnetic energy* 2007 Nov 19: CRC press.
3. Potretzke, T.A., et al., *Microwave versus radiofrequency ablation treatment for hepatocellular carcinoma: a comparison of efficacy at a single center*. *Journal of Vascular and Interventional Radiology*, 2016. **27**(5): p. 631-638.
4. Anupma, M., et al., *Microwave Interstitial Tumor Ablation: New Modality for Treatment of Liver Cancer*. *depression*, 2009. **2**: p. 3.
5. Maini, S. *Design optimization of tapered cap floating sleeve antenna for interstitial microwave ablation for liver tumor*. in *2016 IEEE International Conference on Consumer Electronics (ICCE)*. 2016. IEEE.
6. Gas, P., *Transient Analysis of Interstitial Microwave Hyperthermia Using Multi-Slot Coaxial Antenna*, in *Analysis and Simulation of Electrical and Computer Systems* 2015, Springer. p. 63-71.
7. Rattanadecho, P. and P. Keangin, *Numerical study of heat transfer and blood flow in two-layered porous liver tissue during microwave ablation process using single and double slot antenna*. *International Journal of Heat and Mass Transfer*, 2013. **58**(1-2): p. 457-470.
8. Lara, J.E., et al. *Modeling of electromagnetic and temperature distributions of an interstitial coaxial-based choked antenna for hepatic tumor microwave ablation*. in *2015 12th International Conference on Electrical Engineering, Computing Science and Automatic Control (CCE)*. 2015. IEEE.
9. Islam, M.M. and M.A. Islam, *Radio Frequency Ablation of Liver Tumor-Influence of Vein Wall and Location of Large Vessels*. *Journal of Biomedical Engineering and Medical Imaging*, 2017. **4**(6): p. 23-23.
10. Cepeda Rubio, M.F.J., et al., *Coaxial slot antenna design for microwave hyperthermia using finite-difference time-domain and finite element method*. *The Open Nanomedicine Journal*, 2011. **3**(1).
11. Balanis, C.A., *Modern antenna handbook* 2008: John Wiley & Sons.
12. CST, C.S.T., *CST STUDIO SUITE*, 2017, CST Computer Simulation Technology AG: Germany.
13. database, D.-I.-. *3D-IRCAdb-01 database*
14. Gabriel, S., R. Lau, and C. Gabriel, *The dielectric properties of biological tissues: III. Parametric models for the dielectric spectrum of tissues*. *Physics in Medicine & Biology*, 1996. **41**(11): p. 2271.
15. Maini, S. and A. Marwaha. *Microwave Interstitial Thermal Ablation of Hepatic Tumors by Extended Tip Sliding Choke Antenna*. in *2011 Fourth International Conference on Emerging Trends in Engineering & Technology*. 2011. IEEE.

16. Mital, M. and R.M. Pidaparti, *Breast tumor simulation and parameters estimation using evolutionary algorithms*. Modelling and simulation in engineering, 2008. **2008**.
17. Keangin, P., K. Vafai, and P. Rattanadecho, *Electromagnetic field effects on biological materials*. International Journal of Heat and Mass Transfer, 2013. **65**: p. 389-399.
18. Tungjitkusolmun, S., et al., *Three-dimensional finite-element analyses for radio-frequency hepatic tumor ablation*. IEEE transactions on biomedical engineering, 2002. **49**(1): p. 3-9.
19. Paul, A., A. Pla, and L.L. Weng, *Thermal Modeling of Microwave Percutaneous Hepatic Tumor Ablation*.
20. Singh, S. and R. Repaka. *Pre-clinical modelling and simulation of hepatic radiofrequency ablation*. in *Proc COMSOL Conference 2015*. 2015.
21. Fang, Z., et al., *Design of a novel electrode of radiofrequency ablation for large tumors: a finite element study*. Journal of Engineering and Science in Medical Diagnostics and Therapy, 2018. **1**(1).
22. Zhang, B., et al., *Numerical analysis of the relationship between the area of target tissue necrosis and the size of target tissue in liver tumours with pulsed radiofrequency ablation*. International Journal of Hyperthermia, 2015. **31**(7): p. 715-725.
23. Chaichanyut, M. and S. Tungjitkusolmun, *Microwave ablation using four-tine antenna: effects of blood flow velocity, vessel location, and total displacement on porous hepatic cancer tissue*. Computational and mathematical methods in medicine, 2016. **2016**.
24. DeBerardinis, R.J. and N.S. Chandel, *Fundamentals of cancer metabolism*. Science advances, 2016. **2**(5): p. e1600200.
25. Gorbach, A.M., et al., *Intraoperative infrared functional imaging of human brain*. Annals of neurology, 2003. **54**(3): p. 297-309.
26. Marieb, E.N. and K. Hoehn, *Human anatomy & physiology*. Ninth Edition ed2013: Pearson education.
27. Yacoob, S.M. and N.S. Hassan, *FDTD analysis of a noninvasive hyperthermia system for brain tumors*. Biomedical engineering online, 2012. **11**(1): p. 1-22.
28. Nizam-Uddin, N. and I. Elshafiey, *Enhanced energy localization in hyperthermia treatment based on hybrid electromagnetic and ultrasonic system: proof of concept with numerical simulations*. BioMed research international, 2017. **2017**.
29. Singh, S., S. Sehgal, and H. Gill, *FEM analysis of microwave hyperthermia and the effect of SAR & temperature elevation on liver tumor*. International Journal of Mechanical and Production Engineering Research and Development, 2017. **3**(4): p. 183-197.